Postprint of: Wołoszyk K., Garbatov Y., Kowalski J., Samson L., Numerical and experimental study on effect of boundary conditions during testing of stiffened plates subjected to compressive loads, ENGINEERING STRUCTURES, Vol. 235 (2021), 112027, DOI: 10.1016/j.engstruct.2021.112027

Numerical and experimental study on effect of boundary conditions during testing of stiffened plates subjected to compressive loads

Krzysztof Woloszyk[a], Yordan Garbatov[b, 1], Jakub Kowalski[a], Leszek Samson[a]

[a] *Faculty of Ocean Engineering and Ship Technology, Gdansk University of Technology, G. Narutowicza 11/12 st., 80-233 Gdansk, Poland*

[b] *Centre for Marine Technology and Ocean Engineering (CENTEC), Instituto Superior Técnico, Universidade de Lisboa, Avenida Rovisco Pais 1049-001 Lisboa, Portugal*

Abstract

The objective of this study is to analyse the effect of boundary conditions during testing on the structural behaviour stiffened plates with different thicknesses subjected to compressive loads. The goal of the compressive tests is to analyse the ultimate strength of a stiffened plate. During the test, relevant physical quantities are measured and investigated. The behaviour of the supporting structure is investigated by analysing the force-displacements relationship and post-collapse shapes of tested specimens. The experimental results are compared with the ones made by FE analyses. The FE model is explored in two variants, considering clamped and simply supported boundary conditions. A detailed comparison of the lateral deflections of plates near the supports is also performed. The analysis has shown that during the test, nearly clamped boundary conditions were achieved, leading to an almost complete restriction of plate rotations during the experimental testing, which complies with the real ship structural behaviour of similar components when deep girders transversally support them.

Keywords: stiffened plate, ultimate strength, FEM, boundary conditions

1 Introduction

The ship hull can be treated as a box girder, composed of the stiffened panels supported by longitudinal and transverse girders. Within the single panel, one can distinguish the series of adjacent stiffened plates. The stiffened plates could be considered as a basic structural component of the ship hull girder, transmitting the longitudinal loads coming from the ship bending, especially in the regions of bottom and deck. There are composed of the stiffener with the attached plating. Thus, various researchers have investigated the ultimate strength of individual stiffened plates [1–3]. In [4], it has been found, that the single stiffened plate subjected to uniaxial thrust will lead to the similar value of ultimate stress as an entire stiffened panel when unloaded edges are left free. For typical aspect ratios of the stiffened plates, the structural behaviour of a single stiffened plate is relatively independent of the adjacent stiffened plates. The analysis of the compressive strength of any stiffened plates allows predicting the ultimate strength of the entire ship hull girder [3]. It provides information about the factors influencing structural pre and post-collapse behaviour. The composition of a ship hull girder, which can be considered as a box-like thin-walled stiffened structure is presented in Figure 1.

[1] Corresponding author e-mail: yordan.garbatov@tecnico.ulisboa.pt; Telf (351) 21 841 7907

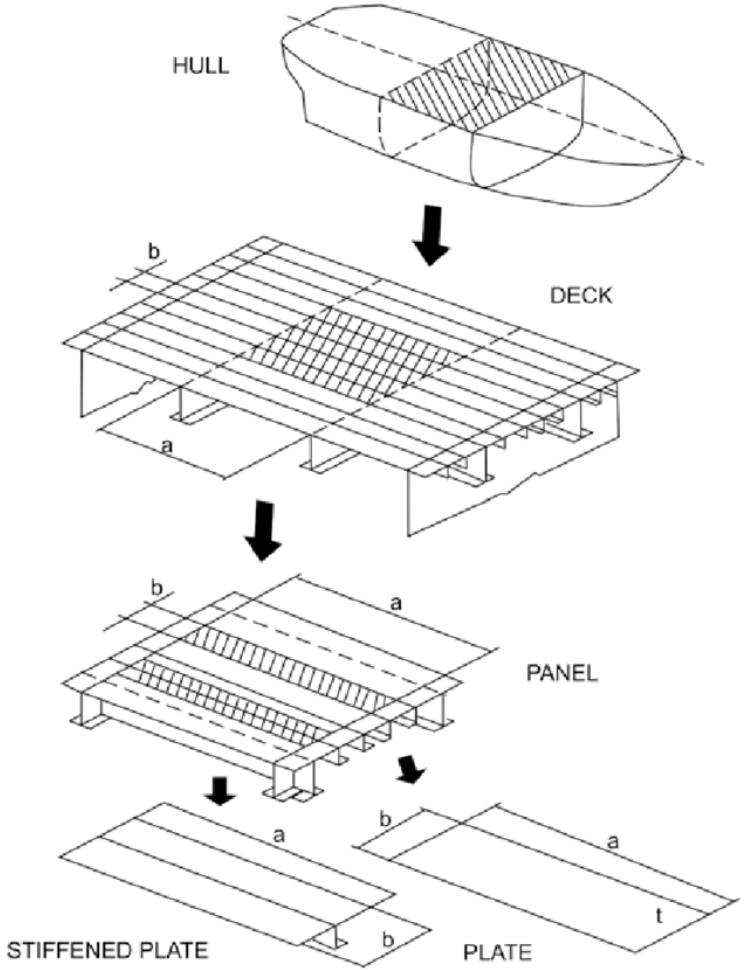

Figure 1. Box-like thin-walled stiffened structure of a ship hull girder [5].

The majority of experimental analyses, concerning the ultimate strength of stiffened plates and panels, were carried out in the 1970s, such as [6–9]. Recently, the series of experiments concerning stiffened panels subjected to axial compressive loads, with the total number of 24 specimens, was carried out by Gordo and Guedes Soares [10–12]. Different column slenderness ratios were investigated as well as stiffener types were analysed. In 2013, the experimental investigation of the ultimate strength of wide stiffened panels was done by Xu and Guedes Soares [13]. Other recent experiments concerning both stiffened plates and panels can be found in [14–17].

The experimental investigations of the ultimate strength of different structural components are still valuable to calibrate the FE analysis and provide information about the uncertainty in terms of future structural reliability analysis [18]. One of the most challenging parts of such experiments is designing the boundary conditions. When plates or stiffened plates subjected to compressive loads are tested, to analyse the structural capacity of ship hull structural components, either simply supported or fixed boundary conditions, are employed. In some recent experimental studies related to intact and aged structures, the simply supported conditions were used in [16,19–22], whereas the clamped supports [23–25]. The simply supported boundary conditions are chosen for several reasons, including the fact that the designing and manufacturing of the experimental stand is more straightforward and because the further validation of the FE analysis with the experimental results gives rather good acceptance. The experimental testing set with clamped boundary conditions, which represents a stiffened plate supported by deep girders, is tough to restrain the cross-sections from rotation and displacement. The

validation of experimental results [24], which was done in [26], revealed that the intended clamped boundary conditions are not behaving ideally. To simulate the plate behaviour during the testing appropriately, the force-dependent boundary conditions were adopted in a FE model leading to good convergence. However, this possibly leads to significant uncertainty and complexity of the FE analysis itself, and the intention is to seek the most straightforward possible solutions for the boundary conditions.

In the case of real ship hull structural components, the stiffened plate is spanned between very deep and stiffer transversal girders, which fixed the edges leading to no displacement and rotation. However, the stiffness is not infinite and allows for some rotation. In the results, as presented in [10], the stiffened panels with different spans and transverse frames were tested and analysed. It was concluded that depending on the stiffener span and transfer girder stiffness, in some cases, the plates behave like fully restrained on the edges. For some other cases, there were more close to simply-supported edges.

The ultimate strength of stiffened plates is related to buckling stresses [1], and the boundary conditions govern it. It is evident that for the clamped stiffened plate, the ultimate strength will be higher than the simply supported one [27]. It seems reasonable to take into account both of these conditions, that will show the lower and upper bound of the ultimate capacity. By taking into account the simply supported constraints, may let to a significant overestimation of the scantling of structural components.

The design of structures subjected to clamped boundary conditions is still challenging. In the study performed in [28], the support-specimen interaction during compressive tests was investigated using a FE analysis. The contact between the specimen edges and the supporting structure was modeled with the use of contact elements. A specially designed support structure was proposed to reduce the gap between the edges and supporting structure. The study revealed that with a maximum aperture of 2 mm, the stiffened plate should behave like a clamped one during testing. This problem is relevant not only in the case of ultimate strength testing, as demonstrated in [29], where the boundary conditions of the dynamic response of tested beams were investigated numerically. The analysis showed the importance of the proper design of specimen mounting supports. In the case of referred studies concerning the experimental testing of ultimate strength, the detailed analysis of boundary conditions behaviour is lacking.

In the presented study, the results of pre-experimental numerical investigations performed in [28] are verified in real experimental conditions. The ultimate compressive tests are performed for three stiffened plates with different thicknesses. To verify the behaviour of loaded edges, four displacement gauges are installed in the corners of the specimen to measure the lateral displacement. The post-collapse shapes of the specimens are also investigated. For each thickness of the stiffened plate, the FE analyses for both simply supported and clamped boundary conditions are carried out and compared with the experimental tests.

2 Experimental set-up

The tested specimens are fabricated with three different thicknesses of 5, 6, and 8 mm as a stiffened plate is presented in Figure 2. The samples were automatically arc welded and there are made from the S235 mild steel (see Figure 2). Three coupons of each thickness were tested to evaluate the material properties, and the mean values of mechanical properties are estimated as presented in Table 1. The coupons were taken from steel sheets that were used to fabricate the specimens as well.

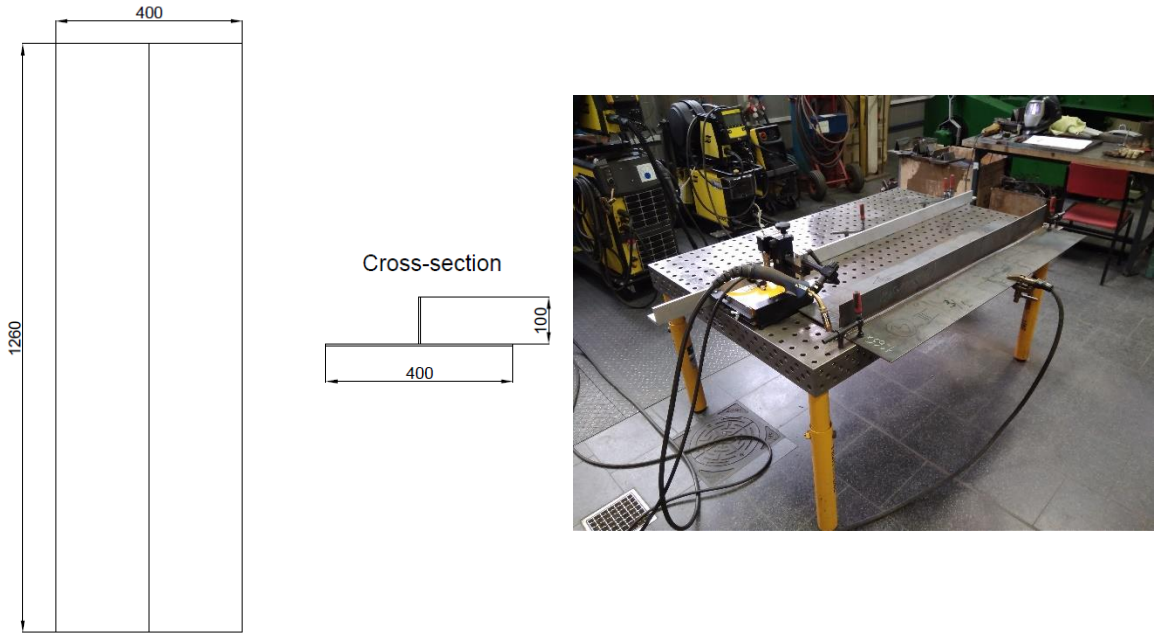

Figure 2. Specimens dimensions (left) and welding process (right).

Table 1. Material properties of the material.

Thickness	Yield stress [MPa]	Young modulus [GPa]	Ultimate tensile stress [MPa]	Total elongation [-]
5	263.2	199.0	386.5	0.278
6	279.3	190.6	404.8	0.267
8	357.5	196.7	457.0	0.224

The designed supports, which were the outcome of the study conducted in [28], are presented in Figure 3. The main feature of the presented supports is they are adjustable to the specimen thickness. Thanks to the steel mounting blocks controlled by the set of screws, the gap between the support and plate may be reduced to the minimum, leading to a fully clamped structures. The study performed in [28] concluded that when the gap between the tested specimen and support is not exceeding 2 mm, the supports create conditions that the structure may be assumed as a fully clamped one. One needs to notice that the effective length of the plate is reduced by 20 cm due to the presence of the supports, and that needs to be accounted for during numerical analysis.

Figure 3. Supports during design phase (left) and in real experiment (right).

The standard testing machine, equipped with a hydraulic pressure system allowing a maximum load of compression of 4,000 kN and tension of 2,000 kN, was used in the experimental testing.

Strain gauges were mounted accordingly to record the strain in the critical locations. Additionally, the mid-lateral displacement was also measured, and the displacements in the four corners of the specimen were measured using displacement gauges. The gauge's distribution is presented in Figure 4. A video camera was used to monitor the deformed shape of the stiffened plate during the testing. The installed strain and displacement gauges may be seen in Figure 5.

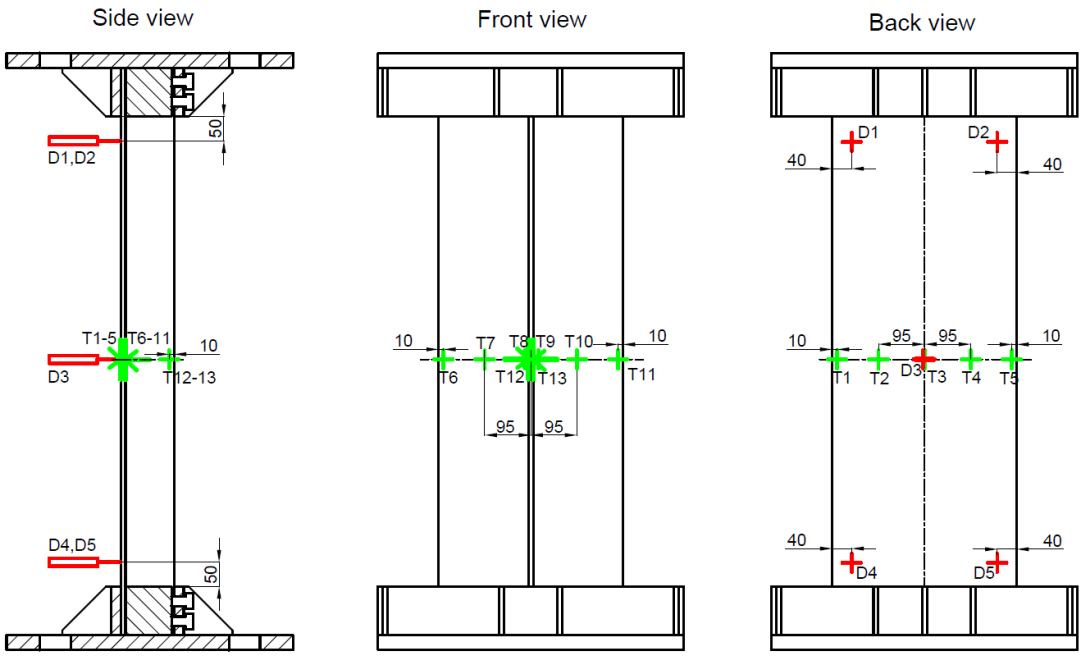

Figure 4. Distribution of strain gauges and displacement transducers (strain gauges – green, displacement gauges – red).

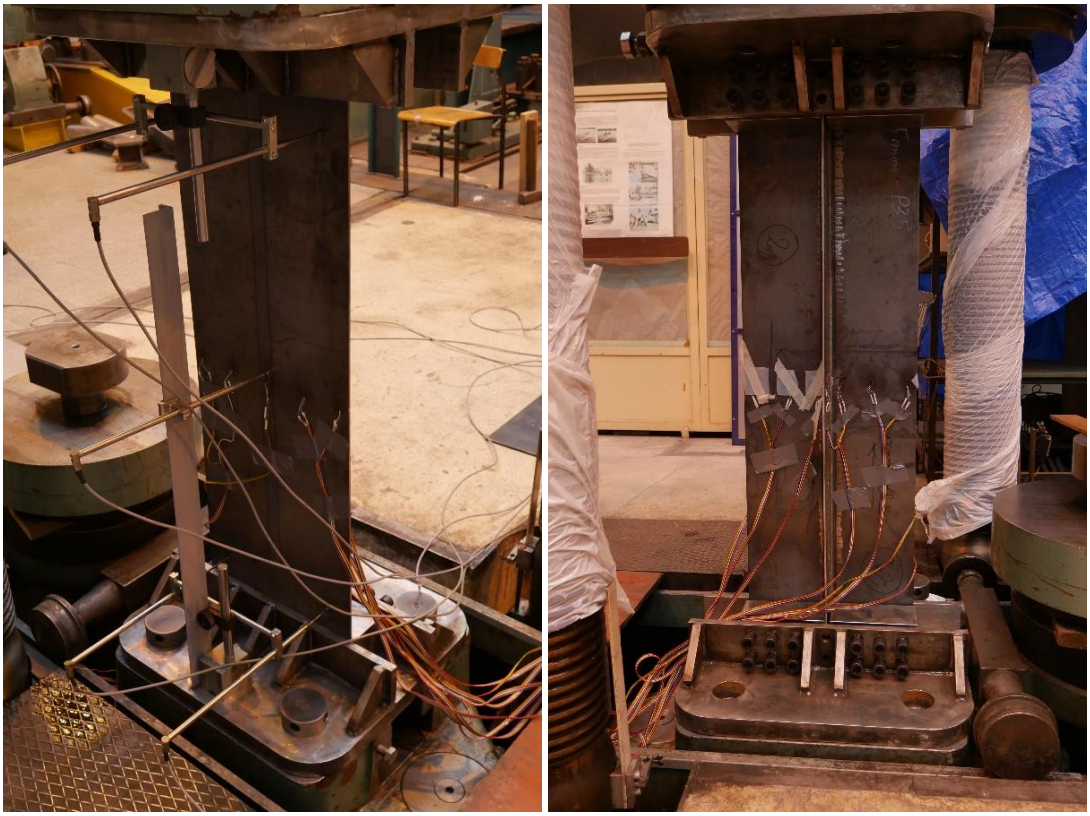

Figure 5. Back (left) and front (right) view of specimen with installed gauges.

3 FE modelling

To verify the structural behaviour of the specimen experimentally, in terms of the boundary conditions, the nonlinear FE analysis is performed using commercial software ANSYS [30]. The static implicit solver considering the Arc-length approach is employed. The eight-node SHELL181 elements are used to model the plate elements. The input material properties are based on the experimental results, as shown in Table 1, and the bilinear material model with hardening is employed. The material properties are different for each thickness. The tangent modulus of linear hardening was considered equal to $E/500$. Both material and geometrical nonlinearities are included in the calculation procedure.

The FE model of the stiffened plate is presented in Figure 6. The boundary conditions are considered in two variants, namely clamped and simply supported one. The applied boundary conditions, referring to edges numbers, as shown in Figure 6, are summarised in Table 2. The loading is developed via an incremental increase of longitudinal displacement of edges 3 and 4.

Table 2. Applied boundary conditions.

Edge number	Simply supported conditions	Clamped conditions
1	$u_x = 0, u_y = 0$	$u_x = 0, u_y = 0, rot_z = 0$
2	$u_z = 0, u_y = 0$	$u_z = 0, u_y = 0, rot_x = 0$
3	$u_x = 0, u_y = coupled$	$u_x = 0, u_y = coupled, rot_z = 0$
4	$u_z = 0, u_y = coupled$	$u_z = 0, u_y = coupled, rot_x = 0$

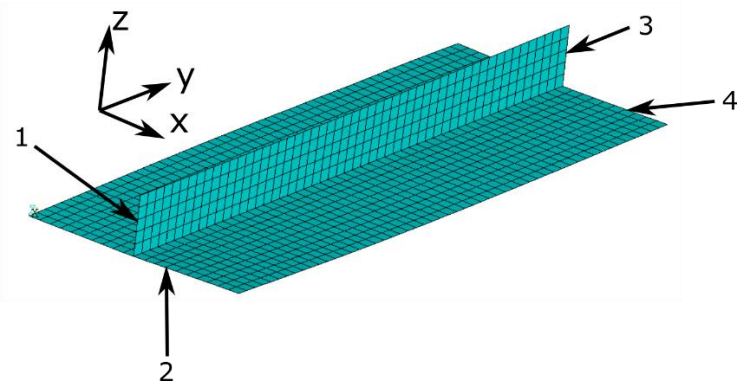

Figure 6. FE model of the stiffened plate.

The initial welding-induced distortions were measured using the photogrammetry technique [31,32] for each specimen, and there were furtherly used as an input for the numerical analysis. The distribution of the initial imperfections is presented in Figure 7, with a scale factor of 5x. The detailed information about the undertaken photogrammetry measurements can be found in [33], which were performed using a camera stand originally designed within the "Mechanics of anterior abdominal wall in optimisation of hernia treatment" national grant (National Science Centre, Poland). The example of the resulting point cloud for one of the specimens and positions where photographs are taken is presented in Figure 8. One could notice, that the specimens clamping could change the level of the initial imperfections of the specimen as presented in Figure 7. In order to identify that, the strains and deflections, as presented in Figure 4 were measured during the clamping procedure, priory to the application of axial loading. There was identified that the imperfections decreased slightly. However, the decrement was marginal concerning to the imperfections level. Thus, it was concluded, that clamping of the specimen won't have a significant impact on the initial specimen state.

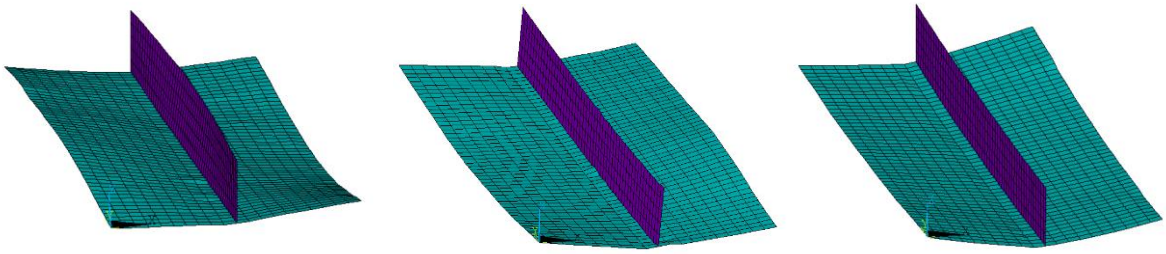

Figure 7. Distribution of initial imperfections of 5 mm (left), 6 mm (mid) and 8 mm (right) specimen (scale factor 5x).

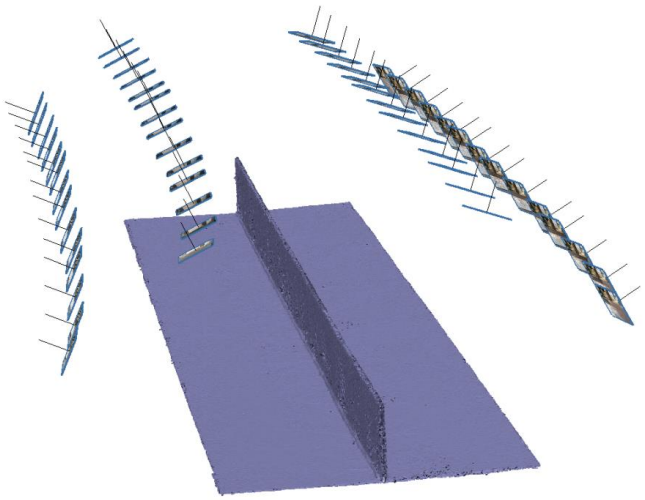

Figure 8. Dense cloud of specimen surface and positions of taken photographs [34].

The mesh convergence studies have been performed, showing that the element size of 20 mm will lead to accurate results.

4 Analysis of boundary conditions

The supports were designed to achieve the clamped boundary conditions leading to no displacement and no rotation. Firstly, the force-displacement relationship from the experiment is compared with the numerical analysis of the linear structural response and eigenvalue buckling, taking into account both clamped as well as simply supported conditions (see Figure 9). However, in the case of experimental results, the displacements at the point where the ultimate strength is reached are significantly higher than the one estimated by the nonlinear FE analysis, which is a common problem observed in different studies, e.g. [21,24]. In the initial stage of the loading (approx. up to the 1 mm of longitudinal displacement), the fluctuations are mainly caused due to the fixation of the specimen in the supports. Initially, both of them are not-ideally matched. However, in the later stage, the experimental force-displacement relationship has much less inclination than the numerical one. The possible reason for that can be that the compressive load applied to the specimen can be non-ideally uniaxial, which cause the eccentricity and an initial secondary bending moment.

However, to compare both strains and displacements, the experimental force-displacement curves have been adjusted to reach the ultimate point at a similar level as the nonlinear FE analysis. The longitudinal displacement measured experimentally has been divided by 2 and 3.5, depending on the specimen.

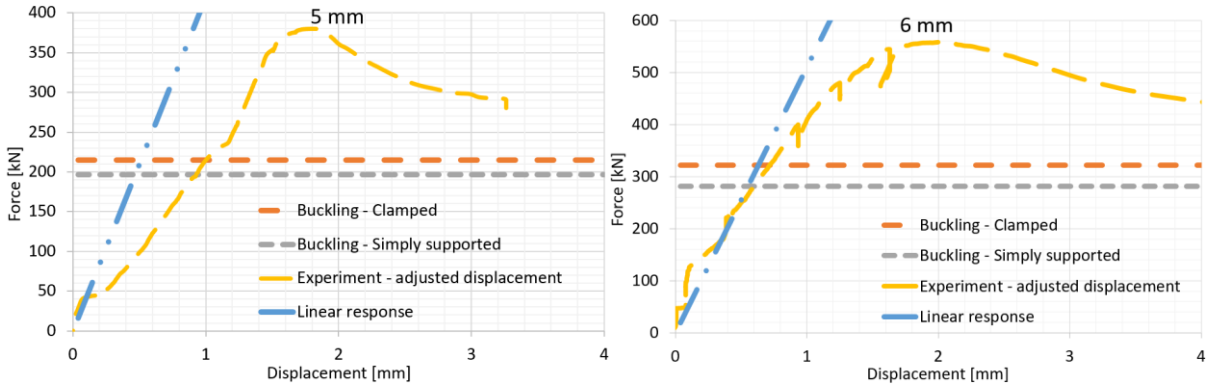

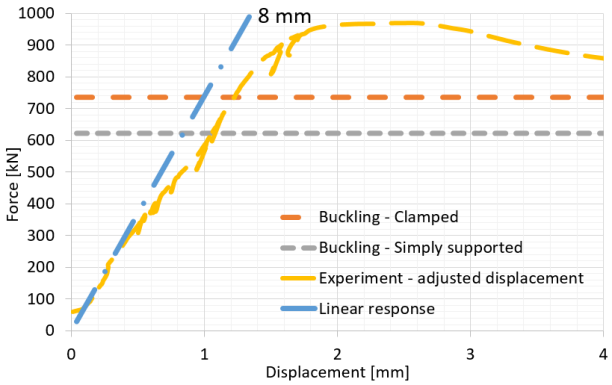

Figure 9. Force – displacement relationship for 5 mm (left up), 6 mm (right up), and 8 mm (bottom) specimen.

From the comparison presented in Figure 9, it is notable that there is no significant difference between critical force for both clamped and simply supported conditions. The reason for that is the restriction of an end-cross section of the stiffened plate from rotation, and the plate can rotate only locally. Due to that fact, the shape of the stiffened plate results in strong support itself, having a significant stiffness. Eventual clamping will additionally restrict the plate from a local rotation near the supports. The differences in the ultimate strength will be much higher for the non-stiffened plate. It could also be noticed that the differences in ultimate strength are even smaller compared to the nonlinear FE analysis (see Table 3). Thus, it may be concluded that the FE analysis predicts the ultimate strength of the stiffened plate accurately, and it is not so sensitive in the local rotation of the plate. The buckling capacity is lower than the estimated ultimate strength. When the elastic buckling occurs, the structural component will still carry out some load to the structural collapse. It is also observed that the initial inclination of the experimental curve is very similar to the linear response obtained in the numerical analysis. However, with the increase of the longitudinal displacement, the bending causing the high deflections of the plate occurs, leading to a drop of the force-displacement curve inclination.

The load-carrying capacity for both experimental and numerical results is very similar, as presented in Table 3. The ultimate load of the FE analysis with clamped boundary conditions is slightly closer to the experimental value. The differences between the simply supported conditions and clamped ones in terms of the FE analysis are increasing with the increase of the thickness. There are reaching about 3 % in the case of an 8 mm specimen thickness.

Table 3. Ultimate force, derived from experimental and numerical analyses.

Thickness [mm]	Ultimate force [kN]			Differences [%]	
	Experiment	Numerical - Simply Supported	Numerical - Clamped	Exp. – Simply Supported	Exp. - Clamped
5	380.2	401.1	403.8	5.5	5.9
6	559.5	528.9	537.2	-5.5	-4.1
8	969.9	950.4	979.7	-2.0	1.0

Furtherly, the post-collapse shapes of tested specimens are investigated. As it was analysed in [28], for the clamped boundary conditions (the gap between the specimen and supporting clamps will be small enough) and simply supported one, the post-collapse forms are quite different, as can be seen in Figure

10, where an example a specimen of a 5 mm specimen thickness is presented. When clamped boundary conditions are employed, the one half-sine wave distortion, during plate buckling loading, occurs. The highest deflections are observed near the mid-cross-section along with the specimen. In simply supported specimens, the two half-sine wave displacement during plate buckling occurs with an excessive amount near the supports.

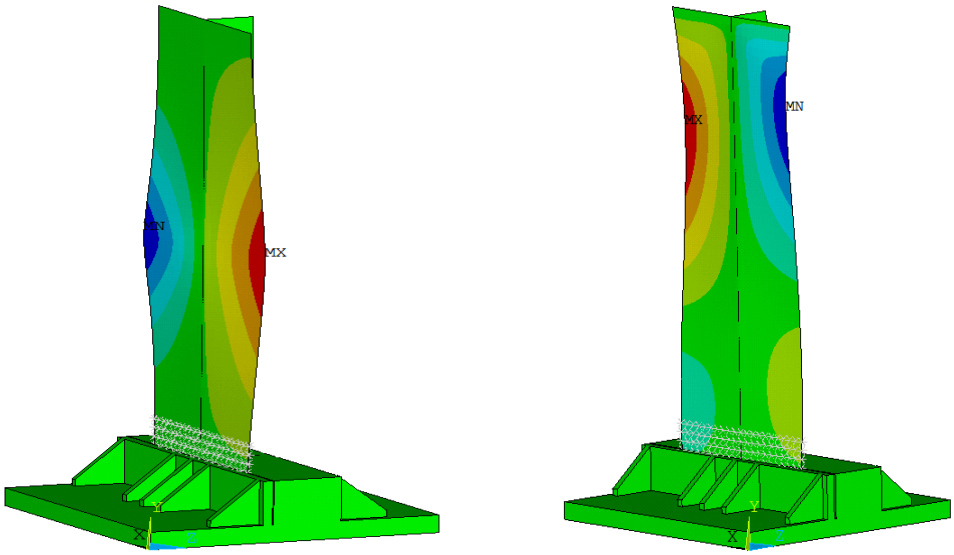

Figure 10. Post-collapse displacement of clamped (left) and simply supported specimens (right) [28].

The post-collapse shapes of the tested specimens are presented in Figure 11. It may be noticed that the shape of the deformed specimens is relatively similar. The collapse has been caused by the local plate buckling followed by stiffener tripping. Global column buckling was not observed. In both 5 mm and 6 mm specimen thicknesses, the cross-section of the highest deflections occurred in some distance from the mid-cross-section, which was not observed in the initial numerical studies. In an 8 mm stiffened plate thickness, the extreme deflections occur very near the mid-cross-section. Furtherly, in all specimens, the one half-sine waves as a result of buckling, which shows that the supports behaved adequately, as it was anticipated in pre-experimental studies.

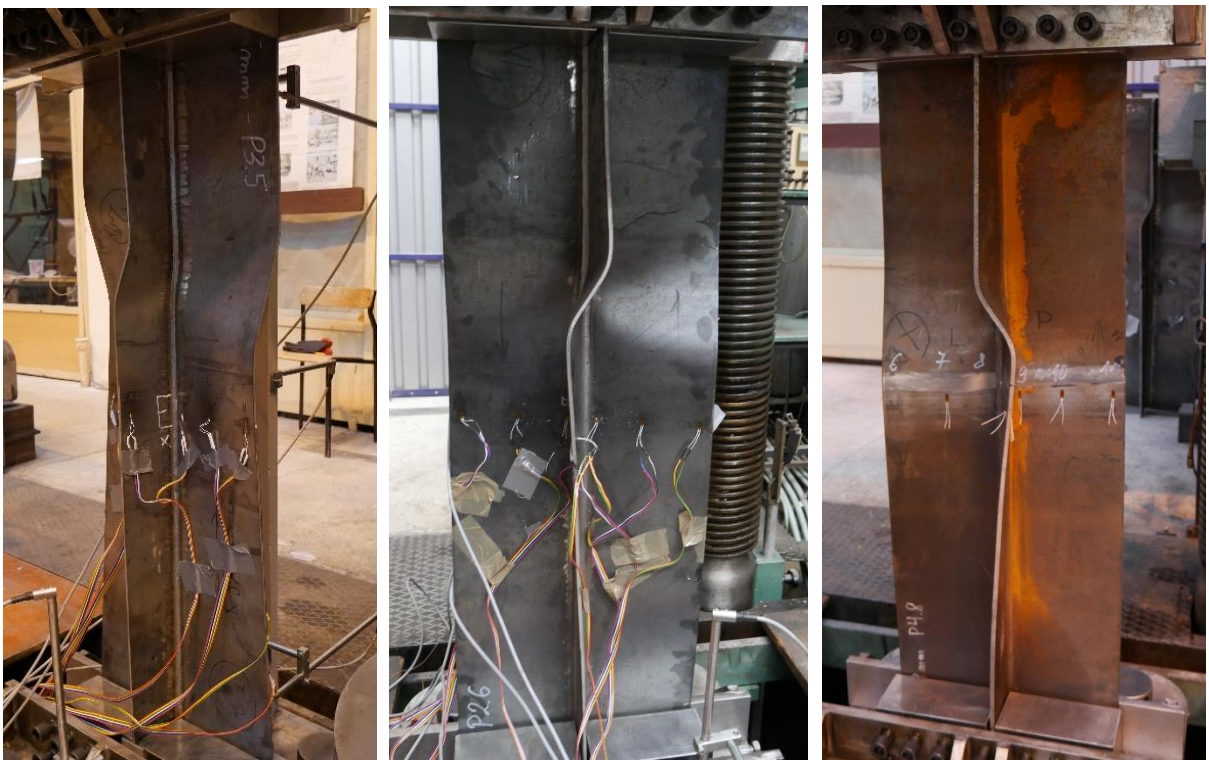

Figure 11. Post-collapse shape for 5 mm (left), 6 mm (mid) and 8 mm (right) specimen thickness - experiment.

The post-collapse shapes are compared with numerical investigations accounting for measured initial imperfections and considering clamped boundary conditions, as presented in Figure 12. In general, the deformation forms from both experimental and numerical studies are similar, i.e., the local plate buckling followed by stiffener tripping caused the collapse of the stiffened plates. The most identical deflection shapes are observed for a 6 mm specimen. In this case, the position of highest deformations is similar and the form of the collapsed stiffener. In the case of a 5 mm specimen, the position of the collapsed cross-section, not the same as in a FE analysis, which results in slightly different shape of both collapsed plate and stiffener.

Regarding the 8 mm specimen, the position of the collapsed cross-section and shape of the collapsed plate are similar, and the only form of the damaged stiffener is different. The differences of post-collapse shapes, as was found in [35], may be as a result of a non-uniform distribution of mechanical properties within a single stiffened plate. Other possible factors that may change the post-collapse behaviour are the welding-induced residual stresses.

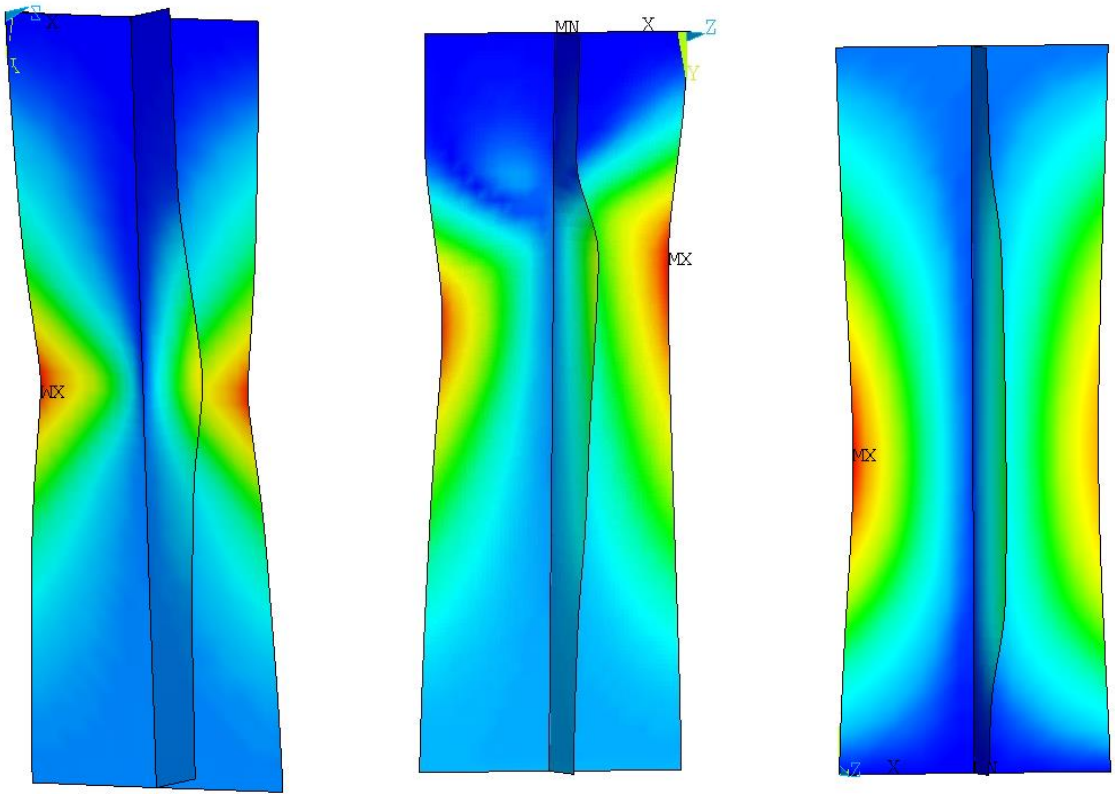

Figure 12. FE post-collapse shape for 5 mm (left), 6 mm (mid) and 8 mm (right) specimen

Based on the analysis of the post-collapse forms of tested specimens, in comparison to pre-experimental FE analyses of supporting structure as well as the stiffened plate accounting for the initial geometrical imperfections, several conclusions may be derived. The designed supports can generate boundary conditions very close to the clamped ones, avoiding buckling forms with several half-sin waves. When comparing tested specimens with a FE analysis, the deformation forms are very similar, although, in the case of 5 mm and 8 mm specimens, some differences are observed.

It may be concluded that the rotations of the stiffened plate cross-sections in the supports were restrained. However, to investigate the clamped condition of plates locally, the lateral displacements near the supports were measured (see Figure 4). When comparing the theoretical shapes of the buckled plate in the case of clamped and simply supported conditions (see Figure 12), one can notice that there are significant differences of the rotation of the edge near the support (φ_1 and φ_2). Actually, in the point of supports, there is no rotation in the case of a clamped plate. When one measures the lateral displacement in very close distance from the support, the rotation of the edge can be estimated as the deflection (w_1 and w_2) divided by the distance d, as it is presented in Figure 12.

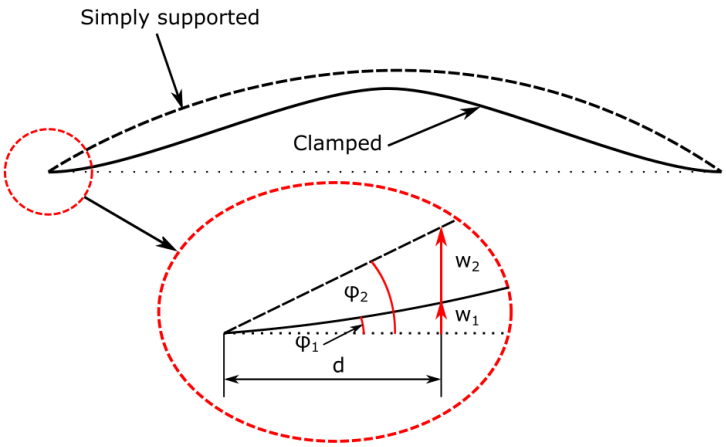

Figure 13. Displacement distribution of equally loaded simply supported and clamped plates.

To validate the boundary conditions, an analysis of the lateral plate displacements near the supports is carried out (d1, d2 (upper edge) and d4, d5 (bottom edge) using the displacement gauges presented in Figure 3). The measurements were compared with the FE analysis considering that the plate and stiffener are simply supported or clamped. The comparison for all lateral displacements in the function of longitudinal displacement for a 5 mm specimen is presented in Figure 14.

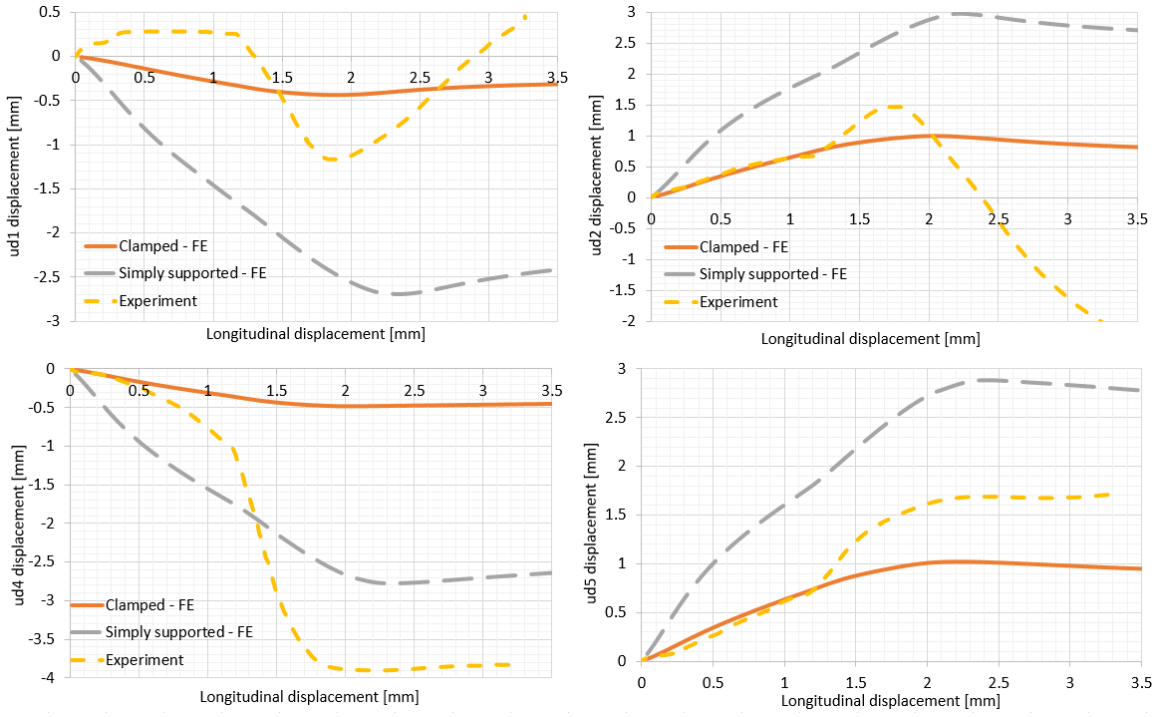

Figure 14. Displacements of the plate near support for 5 mm specimen.

One can notice that up to a 1.25 mm longitudinal displacement produced by a load before reaching the ultimate strength, the edges were almost without rotation. Up to that point, the behaviour was the same as for the FE analysis, considering the fully clamped conditions. After that point, the plate buckled elastically, increasing the deflections near the lower edge and decreasing the deflections near the upper edge. The FE analysis did not capture this phenomenon. Apart from that, the displacements near the supports increased, but still closer to the clamped boundary conditions (ud1, ud2, and ud5). Only in the case of the plate corner (ud4), the displacement increased rapidly. After arriving at 2 mm

longitudinal displacement, where the ultimate bending moment of the critical cross-section is achieved, and the response force starts decreasing, the displacement of the lower edge stabilised on a constant value, similarly to the one of the FE analysis. However, on the upper edge, the displacement started to increase in the opposite direction. The differences between the experimental set-up and FE model are mainly the reason for the different locations of the collapsed cross-section, which was observed in the middle of the specimen in the case of FE analysis. It was more close to the upper support in the case of the tested specimen. Thus, the differences are caused by different post-collapse shapes, governed by many factors, including the boundary conditions. The comparison of the lateral displacements of a 6 mm specimen is presented in Figure 15.

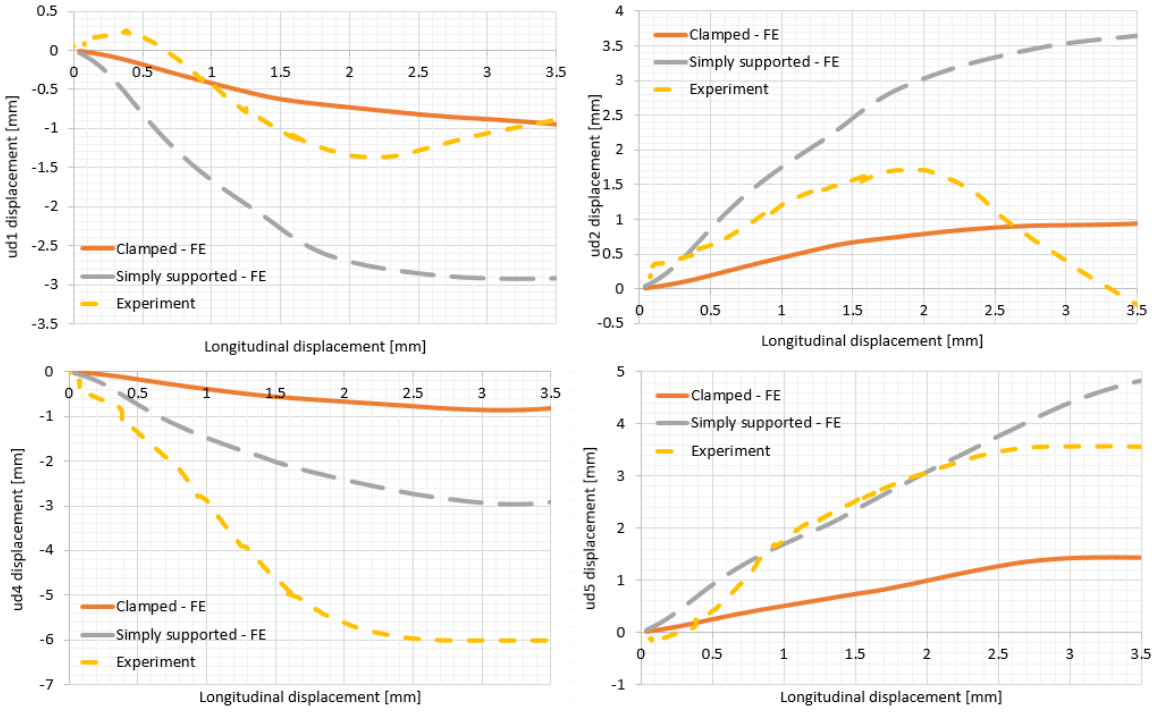

Figure 15. Displacements of the plate near the support for 6 mm specimen.

As can be noticed, in the upper edge (ud1 and ud2, see Figure 4), the boundary conditions are very close to the clamped ones. However, in the bottom edge (ud3 and ud4), the structural behaviour is more comparable to the simply supported conditions. In the case of ud3 measurements, there were even more prominent than the results of the FE analysis considering the simply supported conditions. After reaching the ultimate strength, both displacements stabilised on a constant value. Additionally, in the case of ud2 and ud3 gauges, the notable drop of the displacement at the beginning of the loading process is observed. This may be due to the initial adjustment of the specimen to the support as a result of possible misalignments between the specimen and support.

The comparison of the lateral displacements near the supports for the 8 mm specimen thickness is presented in Figure 16. It can be noticed for all measurements, that for longitudinal displacement between 0 and 0.5 mm, some lateral displacements were captured, which was not observed in the FE analyses either with clamped or simply supported edges. Probably this was the result of an initial plate adjustment to the supports. After reaching that point, in the case of the upper edges (ud1 and ud2), the displacements were very close to the clamped boundary conditions. However, the bottom edge (gauges ud4 and ud5) revealed the behaviour somewhat closer to the simply supported conditions. After reaching the ultimate strength (approx. 2 mm of the longitudinal displacement), the

displacement near the upper edge decreased, whereas the displacement near the bottom edge stabilised on a constant level.

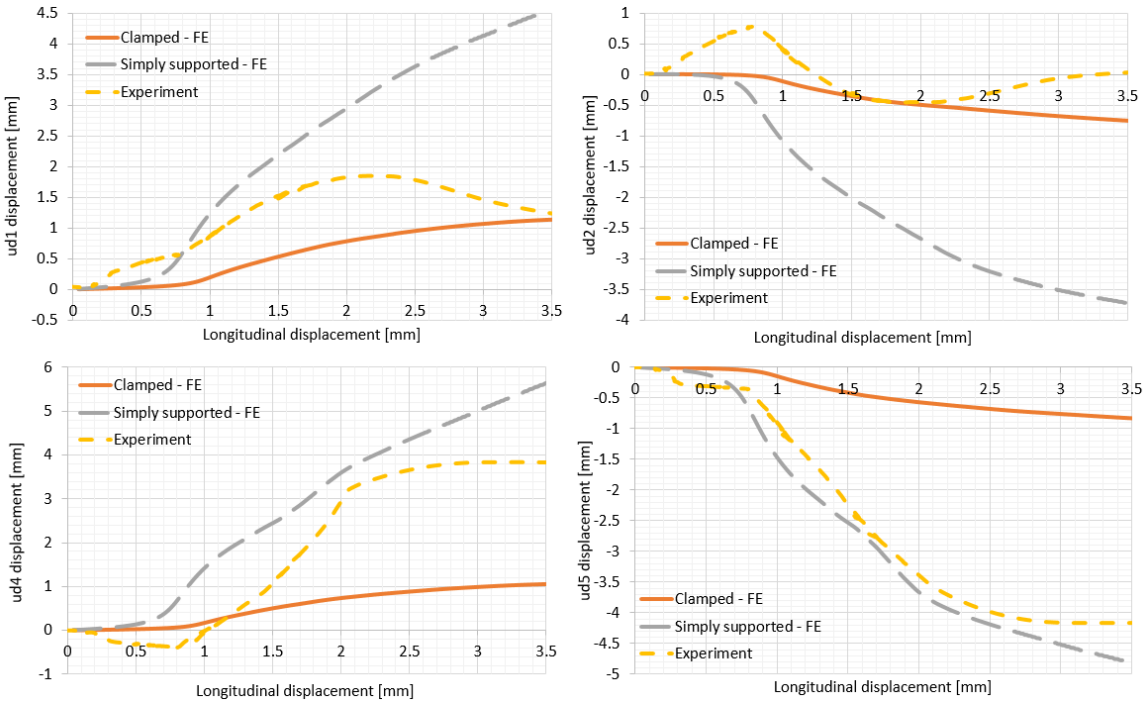

Figure 16. Displacements of plate near the support for 8 mm specimen.

Based on the detailed analysis of the lateral displacements of the plate near the supports, several general observations related to all specimens may be derived. It can be noticed that the displacements near the upper support (ud1 and ud2) were relatively very close to the results of the FE analysis with clamped boundary conditions. However, in the case of displacements near the bottom support (ud4 and ud5), the behaviour was closer to the FE analysis with simply supported boundary conditions. The only exception was the 5 mm specimen, wherein the case of ud5, the displacement was also very close to the clamped boundary conditions. Another phenomenon that was observed for all specimens was that after reaching the ultimate strength, the displacement near the upper support started to decrease.

In contrast, the displacements near the bottom support stabilised on a constant level. Summarising, in all cases, the boundary conditions very close to the clamped ones were achieved, which was the intention of the design. The closest stiffened plate with clamped support behaviour was achieved for a 5 mm specimen. In the case of 6 mm and 8 mm specimens, the bottom support tended to simulate boundary conditions close to the simply supported ones.

One can distinguish many possible reasons that caused the differences between the experimental measurements and FE analyses. Firstly, both plate and stiffener were subjected to some misalignments. Thus, the absolute elimination of the gap between the supports and specimen is unachievable. Secondly, the loading process in the real machine is different from the one generated in the FE analysis. In experimental testing, the incremental loading has been produced by a hydraulic jack-up subjected to in the middle of the bottom support. In the upper support, the load has been transmitted via the upper head placed on the two side columns, leading to a more uniform response distribution in the specimen compared to the bottom edge. This led to the slightly unsymmetrical behaviour for the specimen, which was observed in measuring the lateral plate displacements. In the case of the FE analysis, the incremental loading was identical for both bottom and upper edge of the

specimen. With the increase of loading, another problem related to the testing machine was raised about possible non-perfectly uniaxial loading. This may lead to some eccentricity in loading and introduce an additional bending moment, causing higher lateral displacements of plates. Finally, it needs to be noted that the restraining of rotation in the FE analysis is also challenging.

Figure 17 compares the post-collapse shapes near the support for both FE analysis and tested specimen. It can be noticed that in the case of a FE analysis, the boundary conditions cause the restrain of the edge rotation, and deformed and unreformed edge are covering near the support. However, in the case of the experiment, the excessive lateral displacement of the plate near the mid-length region causes the local plate bending near the support and creates a plastic hinge. One needs to note that the plastic hinge can be considered as a simply supported condition. This explains the differences between the FE analysis and experiment in the lateral plate displacements, as reported in Figures 14 – 16.

The plastic hinges were observed near the bottom support for all specimens. Thus, the total restriction of the plate rotation near the support is impossible to be achieved, even when considering the welding of the transverse edge to the support. Based on that, it could be concluded that the ideal clamped conditions are rather non-achievable in both experimental testing and real ship structures.

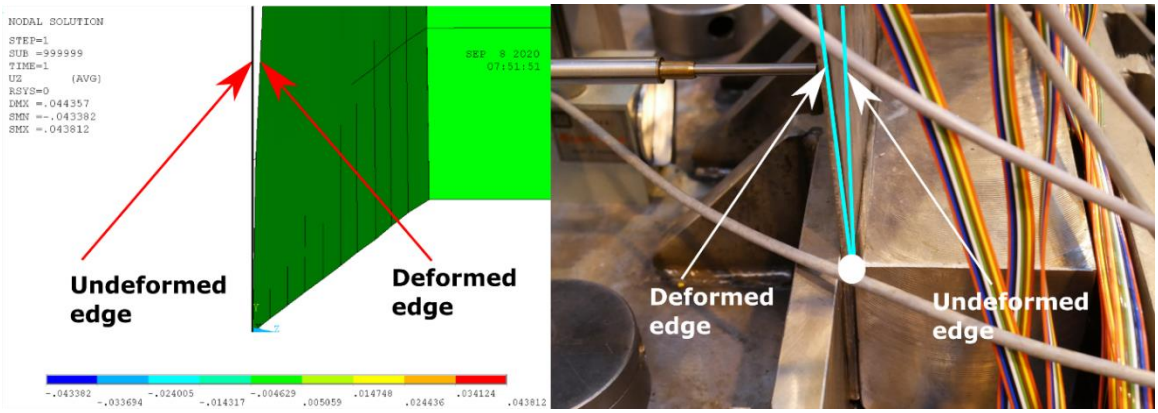

Figure 17. Post-collapse shape of specimen in support region, FE analysis (left), and tested specimen (right).

Conclusions

The presented study investigated the impact of the boundary conditions on the ultimate strength of stiffened plates with different thicknesses during experimental testing. Based on the experimental and FE analyses, several conclusions are derived. The experimental testing aimed to analyse the achievement of the clamped boundary conditions, which was preceded by an advanced FE analysis of the support-specimen structural interaction. The experimentally estimated ultimate strength of the stiffened plate revealed to be very close to the FE analysis considering clamped boundary conditions. Nevertheless, even when the FE analysis considers simply supported conditions, the differences in estimating the ultimate strength is also minimal. The reason is that both of the upper and lower cross-section of the specimen are restrained from out of plate rotation, and the shape of the stiffened plate results in strong support itself. Eventual clamping will additionally restrict the plate from a local rotation near the support. Thus, the developed FE models and performed analyses are credible in representing the experimental testing of the stiffened plate subjected to compressive load. The estimated ultimate strength is very similar compared to the one evaluated by the experiment.

Based on the analysis of the post-collapse shapes, it can be concluded that the gap between the support and specimen has been minimised. In each specimen, the observed buckling shape was the

one half-sine wave of loss of stability. This is consistent with the pre-experimental numerical investigations. Furtherly, similar post-collapse forms were noticed between the FE and experimental analysis, although some differences occurred. Based on that, it was concluded that the clamped boundary conditions were achieved. In each specimen, the local plate buckling, followed by stiffener tripping, was identified as a reason for the structural capacity loss.

The detailed analysis of lateral plate deflections near the supports and comparison with the FE analyses with both clamped and simply supported boundary conditions revealed that fully-clamped conditions were not achieved. Several possible reasons were identified, including the non-ideal force transition via the testing machine, the possible eccentricity of axial loading, the unfairness of both stiffened plate and supporting structure. Furtherly, by comparing the post-collapse shapes of specimens near the support, it was concluded that the total restriction of the plate rotation is challenging in experimental conditions, leading to the possible creation of plastic hinges. This will be valid also when one considers the real ship's structural stiffened plates.

Finally, it is concluded that the clamped boundary conditions, as defined in the present study, have been achieved in terms of restraining the stiffened plate cross-sections from rotation in the supports. However, for some specimens, the plates were not fixed ideally in terms of local plate buckling, which will also be observed in real ship structures. The main advantage of the present support design is that it provides very stable support without welding. It is easily adjustable to specimens with different thicknesses and provides simplicity during specimen's replacement. The FE analysis with clamped boundary conditions can predict the ultimate strength of stiffened plates with sufficient accuracy. However, it is noted that in real situations, the fully-clamped conditions will not occur either.

In presented work, only measurements crucial for the proposed boundary conditions' effectiveness are presented, compared with numerical simulations and discussed. The analysis of measurements obtained from strain gauges, comparison between force-displacement curves, and comparison with other empirical formulations was presented in [35], together with measurements and discussion about residual welding stresses' impact. The model has been compared with the approach from Common Structural Rules [36], which is used to evaluate hull girder ultimate strength in design, based on the stress-strain responses of the stiffened plate elements treated separately. The study revealed that the design formulations are non-conservative with comparison to the presented model.

Acknowledgements

This work has been supported by the National Science Centre, Poland (grant No. 2018/31/N/ST8/02380). The ANSYS software used in presented simulations in this paper was available as a part of the partnership cooperation agreement between ANSYS Inc., MESco sp. z o.o., and the Gdansk University of Technology.

Disclosure statement

The authors reported no potential conflict of interest.

References

[1] Gordo JM, Guedes Soares C. Approximate method to evaluate the hull girder collapse strength. Mar Struct 1996;9:449–70.

[2] Tekgoz M, Garbatov Y, Guedes Soares C. Ultimate strength assessment of welded stiffened plates. Eng Struct 2015;84:325–39.

[3] Yao T, Fujikubo M. Buckling and ultimate strength of ship and ship-like floating structures. 2016.

[4] Tanaka S, Yanagihara D, Yasuoka A, Harada M, Okazawa S, Fujikubo M, et al. Evaluation of ultimate strength of stiffened panels under longitudinal thrust. Mar Struct 2014;36:21–50.

[5] Khedmati MR, Ghavami K, Rastani M. A comparative study on three different construction methods of stiffened plates-strength behaviour and ductility characteristics. Rem Rev Esc Minas 2007;60:365–79.

[6] Smith C. Compressive strength of welded steel ship grillages. Trans RINA 1975;118:325–59.

[7] Faulkner D. Compression tests on welded eccentrically stiffened plate panels. In: Dowling P, editor. Steel plated Struct., London: Crosby Lockwood Staples; 1977, p. 581–617.

[8] Horne M, Narayanan R. Ultimate capacity of stiffened plates used in girders. Proc Inst Civ Eng 1976;61 (Part 2:253–80.

[9] Dorman A, Dwight J. Tests on stiffened compression panels and plate panels. Int. Conf. Steel Box Girder Bridg., London: Institutes of Civil Engineers; 1973, p. 63–75.

[10] Gordo JM, Guedes Soares C. Compressive tests on short continuous panels. Mar Struct 2008;21:113–37.

[11] Gordo JM, Guedes Soares C. Compressive tests on stiffened panels of intermediate slenderness. Thin-Walled Struct 2011;49:782–94.

[12] Gordo JM, Guedes Soares C. Compressive Tests on Long Continuous Stiffened Panels. J Offshore Mech Arct Eng 2012;134.

[13] Xu MC, Guedes Soares C. Experimental study on the collapse strength of wide stiffened panels. Mar Struct 2013;30:33–62.

[14] Kwon YB, Park HS. Compression tests of longitudinally stiffened plates undergoing distortional buckling. J Constr Steel Res 2011;67:1212–24.

[15] Choi BH, Hwang M, Yoon T, Yoo CH. Experimental study of inelastic buckling strength and stiffness requirements for longitudinally stiffened panels. Eng Struct 2009;31:1141–53.

[16] Manco MR, Vaz MA, Cyrino JCR, Ramos NM, Liang DA. Experimental and numerical study of uniaxially compressed stiffened plates with different plating thickness. Thin-Walled Struct 2019;145:106422.

[17] Paik JK, Lee DH, Noh SH, Park DK, Ringsberg JW. Full-scale collapse testing of a steel stiffened plate structure under cyclic axial-compressive loading. Structures 2020;26:996–1009.

[18] Czujko J, Bayatfar A, Smith M, Xu M, Wang D, Lützen M, et al. Committee III.1: Ultimate Strength. In: Kaminski M, Rigo P, editors. Proc. 20th Int. Sh. Offshore Struct. Congr. (ISSC 2018) Vol. 1, IOP Press; 2018, p. 335–439.

[19] Zhang J, Shi XH, Guedes Soares C. Experimental analysis of residual ultimate strength of stiffened panels with pitting corrosion under compression. Eng Struct 2017;152:70–86.

[20] Shi XH, Zhang J, Guedes Soares C. Experimental study on collapse of cracked stiffened plate with initial imperfections under compression. Thin-Walled Struct 2017;114:39–51.

[21] Kim U-N, Choe I-H, Paik JK. Buckling and ultimate strength of perforated plate panels subject to axial compression: experimental and numerical investigations with design formulations. Ships Offshore Struct 2009;4:337–61.

[22] Paik JK, Satish Kumar YV, Lee JM. Ultimate strength of cracked plate elements under axial compression or tension. Thin-Walled Struct 2005;43:237–72.

[23] Saad-Eldeen S, Garbatov Y, Guedes Soares C. Experimental investigation on the residual strength of thin steel plates with a central elliptic opening and locked cracks. Ocean Eng 2016;115:19–29.

[24] Garbatov Y, Tekgoz M, Guedes Soares C. Experimental and numerical strength assessment of stiffened plates subjected to severe non-uniform corrosion degradation and compressive load. Ships Offshore Struct 2017;12:461–73.

[25] Zhang Y, Huang Y, Wei Y. Ultimate strength experiment of hull structural plate with pitting corrosion damage under unaxial compression. Ocean Eng 2017;130:103–14.

[26] Woloszyk K, Kahsin M, Garbatov Y. Numerical assessment of ultimate strength of severe corroded stiffened plates. Eng Struct 2018;168:346–54.

[27] Timoshenko SP, Gere JM. Theory of elastic stability. 1961.

[28] Woloszyk K, Garbatov Y. FE analysis of support-specimen interaction of compressive experimental test. In: Georgiev P, Soares CG, editors. Sustain. Dev. Innov. Mar. Technol., CRC Press; 2019, p. 423–8.

[29] Villavicencio R, Guedes Soares C. Numerical modelling of the boundary conditions on beams stuck transversely by a mass. Int J Impact Eng 2011;38:384–96.

[30] ANSYS. Online Manuals, Release 19 2019.

[31] Luhmann T. Close range photogrammetry for industrial applications. ISPRS J Photogramm Remote Sens 2010;65:558–69.

[32] Chen BQ, Garbatov Y, Guedes C. Measurement of weld-induced deformations in three-dimensional structures based on photogrammetry technique. J Sh Prod 2011;27:51–62.

[33] Woloszyk K, Bielski PM, Garbatov Y, Mikulski T. Photogrammetry image-based approach for imperfect structure modelling and FE analysis. Ocean Eng 2021;223:108665.

[34] Woloszyk K, Bielski P, Garbatov Y, Mikulski T. Photogrammetry image-based approach for imperfect structure modeling and FE analysis. Submitt Publ 2020.

[35] Woloszyk K, Garbatov Y. Ultimate strength of stiffened plates subjected to

compressive load and spatially distributed mechanical properties. Proceeding MARTECH 2020, 2020, p. (accepted for print).